DIRECT MEASUREMENT OF ENTRAINMENT IN REACTING/NON-REACTING TURBULENT JETS USING PIV

Donghee Han, Raymond M. C. Miraflor and M. Godfrey Mungal
Department of Mechanical Engineering
Stanford Univerisity
Stanford, CA 94305-3032, USA

ABSTRACT

The entrainment into a turbulent jet in coflow is directly measured using Particle Image Velocimetry (PIV). The direct measurement technique is verified by comparing with the measurement with previous results for free jets. By measuring the velocity from the outside of the main jet, the entrainment measurement does not suffer from density fluctuations in reacting jets. The effects of coflow speed, heat release and buoyancy on the entrainment rate are investigated. The increase in coflow speed reduces the entrainment for both reacting and non-reacting jets. Heat release suppresses entrainment by a factor of 2.6 when compared to the non-reacting jet, but buoyancy recovers the entrainment to a faster rate. Therefore, for the initial part of a reacting jet where the jet is momentum driven, heat release has dominant effect on entrainment, but buoyancy compensates the reduction further down-stream of the jet.

INTRODUCTION

Entrainment is the radial inward flux of ambient fluid drawn into a turbulent jet. The rate of entrainment controls the mixing rate of the jet with the ambient and consequently, controls the chemical reaction rate. Therefore, the entrainment to the jet is of fundamental interest, not only in terms of the mixing itself, but as the controlling factor for the pollutant formation in a reacting jet (Broadwell and Lutz, 1998).

The entrainment of the turbulent free jet was carefully studied by Ricou and Spalding (1961) who used a specially designed chamber to directly measure the gross amount of entrained flux into the jet. From the measurement of the non-reacting jet with different densities, they have obtained a simple relation for the entrainment in the momentum driven region, which can be expressed as,

$$\dot{m}/\dot{m}_0 = C_e(x/d^*) \qquad (1)$$

where $\dot{m}$ is the jet mass flux, $\dot{m}_0$ is the initial jet mass flux and x is the downstream distance. d^* is the density weighted nozzle diameter given as, $d_0(\rho_0/\rho_\infty)^{1/2}$. In their work, d^* was found to be the proper length scale to normalize the axial direction, x, for jets with different densities. The entrainment coefficient C_e was determined to be 0.32 for momentum driven free jets. Hill (1972) used the same direct measurement method as Ricou and Spalding, but resolved the entrainment coefficient at different axial positions. He found that the entrainment coefficient grows from low value at the nozzle exit to 0.32 within 13 jet diameters. Becker and Yamazaki (1978) extended the study to include the effect of buoyancy in reacting jets. In their result, they measured the entrainment coefficient, C_e, to be higher than 2.0 in the highly buoyant region, which is more than 6 times larger than the momentum driven extreme. Muñiz (1999) also studied the effect of heat release and buoyancy on entrainment in reacting jets in coflow and found that heat release and existence of coflow reduce the entrainment.

Summarizing the previous studies, we can conclude that the entrainment coefficient defined in equation (1) is not a constant, but a function of many parameters including heat release, buoyancy, coflow speed and position. In this study, a direct entrainment measurement technique using Particle Image Velocimetry (PIV) is performed for both reacting and non-reacting jets in coflow and the effects of coflow speed, heat release and buoyancy on entrainment are investigated.

EXPERIMENTAL METHOD

In this study, we propose a direct measurement method for measurement of entrainment. Direct measurment of entrainment was first performed by Ricou and Spalding (1961) with a specially-designed cylindrical porous chamber. Their apparatus measured an average entrainment along the length of the

cylinderical chamber they were using. Therefore, the entrainment rate change along the axial position was not measurable. Hill (1972) used the same method, but with the cylinder chamber that can be moved along the axial position so that the change in entrainment can be measured. These direct measurements are effective in the free jet configuration, but cannot be applied to the jet in coflow configuration, which is used in common burner systems. Becker and Yamazaki (1978) measured the impact pressure and average temperature profile along the jet to infer the entrainment. But, their impact pressure measurement includes two unknown terms, $\overline{\rho}\,\overline{u'^2}$ and $\overline{u}\,\overline{\rho' u'}$. These terms can be a significant portion of the total impact pressure especially at jet boundaries, which leads to the error in entrainment estimates. Muñiz used PIV to measure the velocity profile directly, but also had an unknown term, $\overline{\rho' u'}$, which is caused from the density fluctuations in reacting jets. Therefore, the density fluctuation has to be measured simultaneouly with the velocity to obtain accurate entrainment rates using the profile measurement inside the reacting jet. To avoid these difficulties, we need a direct measurment method such as that of Ricou and Spalding, but without the physical structure that intrudes into the flow.

Direct Measurement using PIV

PIV is now a standard technique to measure 2 dimensional velocity fields. The use of a digital camera and computerized velocity processing enhanced the technique significantly (Westerweel, 1997) that we can easily obtain hundreds of velocity fields in each position of interest. The direct entrainment measurement method proposed here uses PIV to measure the velocity field surrounding the main jet. Figure 1 shows the schematic of the process. The average of over 100 velocity fields is then numerically integrated through the control volume as shown in Fig. 1 to extract the entrainment.

If we assume the surrounding fluid is of infinite amount and the wall of the tunnel is far enough not to have any influence, the measurement position should not affect the the entrainment measurement. But, since the surrounding fluid is often limited by the size of the tunnel and the tunnel wall is in a finite distance away, the coflow cannot be assumed uniform along the tunnel in the presence of the jet. Also the radial component of the velocity decays with $1/r^2$ so that it gets too small to measure accurately from far outside of the jet. Therefore, to reduce the error caused by the local depletion of the coflow and radial decay of velocity, we have measured the velocity field as close to the jet boundary as possible. We then have to determine the angle of the jet boundary through which the surrounging fluid is actually entrained. The rough angle measurement can be perfomed using the RMS v' contour image which is found to be a good representation of the jet boundary (shown in Fig. 6, see later). The angle is slightly adjusted after, to make slightly different planes of integration give similar entrainment. The value obtained from 10 different planes with height of 2.5~5cm, separated by about 1.5cm in radial direction, are averaged to give the final entrainment value.

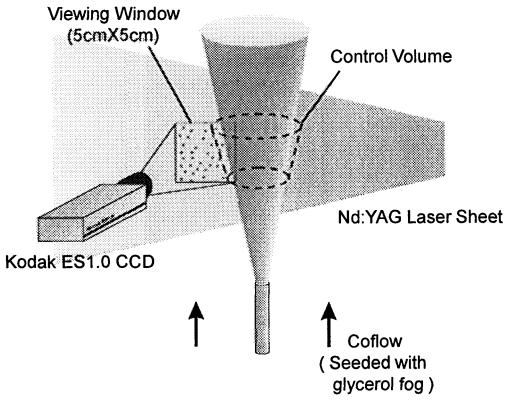

Figure 1. Schematic diagram of direct measurement of entrainment using PIV.

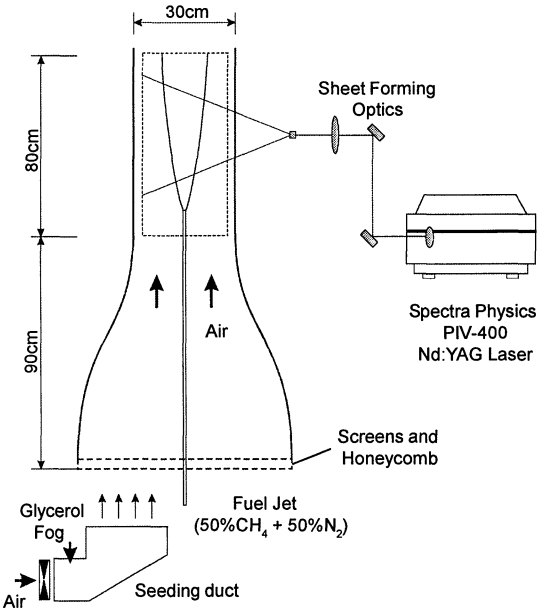

Figure 2. Schematic diagram of experimental apparatus.

Experimental Apparatus

The jet originates from a long tube ($L/d > 300$) of inner diameter 4.6mm, which is centered in the vertical wind tunnel. A concentric tube with a slightly larger inner diameter (7.7mm) supplies a hydrogen pilot to stabilize the flame at the nozzle. The main jet is composed of equal mole fractions of methane (99% purity) and nitrogen. An air jet is also used for the verification of method. Table 1 summarizes the operating conditions that are investigated in this study. The tunnel has a rectangular test section with cross sectional area of 30cm×30cm and height of 80cm. In addition to the honeycomb and screens

TABLE 1. OPERATING CONDITIONS

R	C	Re_d	$10^4\dot{m}_0$ [kg/s]	$10^4\dot{m}_{CF}$ [kg/s]	$\dot{m}_{Hz}/\dot{m}_0$	u_0 [m/s]	u_{CF} [m/s]	r	L_{flame} [cm]	$10^5 Ri_s$	ξ_L
	□	18000	11.86	263		59	0.25	240			
●	○	18000	9.41	526	0.017	62	0.5	109	55	1.04	2.95
▲	△	18000	9.41	1053	0.017	62	1.0	55	57	1.04	3.06
▼	▽	18000	9.41	2106	0.017	62	2.0	27	60	1.04	3.22
◆		9000	4.82	526	0.014	31	0.5	56	48	4.03	4.04

R : Reacting C : Non-Reacting □ : Air Jet

in the inlet, the tunnel has 4 to 1 contraction for conditioning of the flow. The coflow speed can be controlled by changing the angle of a damper located far away from the test section. The schematic of the tunnel is shown in Fig. 2.

For the PIV system, a Kodak ES 1.0 digital CCD array (1016×1008) and Spectra Physics PIV-400 Nd:YAG laser are used. TSI Insight 1.21 software is used to aquire the images with the time delay between laser pulses controlled by a SRS DG 535 delay generator. The coflow is seeded with the glycerol particles using a specially-designed 90° duct for uniform seeding.

The images are processed with the STANPIV code developed by Hasselbrink (1999) which is a cross-correlation code with box offset. The use of the box offset is known to not only increase the detectivity but also reduce the RMS error induced in PIV (Westerweel et al., 1997). Since we only need average values and not a high degree of spatial resolution, the interrogation box size is set to 64×64 pixels with the entire viewing window size of 5cm×5cm. We use 50% overlap for all the interrogation region, and therefore obtain 30 vectors in each direction of the viewing window.

Error Estimation

The sources of error in the direct measurement method can be summarized as: 1) PIV error, 2) error related to the determination of the jet boundary and angle, 3) error due to the uncertainty in position and 4) uncertainty in symmetry.

The RMS error of PIV for the normal cross-correlation, with particle size of 2 pixels and interrogation window size of 32×32, can be as high as 0.1 pixel (Westerweel et al., 1997). But, since we use the box offset which reduces the RMS error and use only the averaged velocity field, the generic PIV error will not be a significant source of error for this experiment.

The error related to the determination of the jet boundary and angle can be significant especially for the cases with relatively large coflow speeds. In all cases we estimated ±10% relative error in angle measurement, which leads to about ±6% error in entrainment rate.

The last source of error which is the uncertainty in position comes from the fact that it is not possible to locate the relative position of the PIV window exactly with respect to the nozzle position. The error increases as we go further to the downstream. The maximum estimated error, which is 5mm uncertainty in 100 jet diameters down stream, causes about ±3% error in entrainment measurement.

Another uncertainty in the measurement is the symmetry of the jet. Since the tunnel is rectangular, it can be possible that the jet is not perfectly axisymmetric. For this study, we assume the jet is perfectly axisymmetric and neglect any asymmetric effect which might exist.

Summarizing all the effects, the relative error of the direct measurement method can be estimated to be within ±10% up to about 100 jet diameters downstream.

RESULTS AND DISCUSSIONS

The experimental method is first verified by measuring the entrainment of a non-reacing jet with very small coflow velocity. We then present the results for non-reacting and reacting jets with different coflow speeds.

Experimental Verification

A non-reacting air jet with exit velocity of 59m/s is injected in a coflow of 0.25m/s. Since the coflow speed is about 1/240 of the jet speed, we expect to have similar behavior with the free jet up to the point where it feels confinement. Figure 3(a) shows the change in the entrainment coefficient along the axial position. Figure 3(b), which is the actual change in mass flux, is obtained by integrating the fitted curve shown in Fig. 3(a).

We can observe the entrainment coefficient approaches 0.32 which is the free jet value obtained by Ricou and Spalding (1961). The same kind of measurement done by Hill (1972) shows that the jet reaches the free jet value within 13 jet diameters downstream while our result converges to the free jet value in about 35 jet diameters.

One major difference in these two measurements are the jet initial configurations. The jet measured by Hill (1972) was originating from a convergent nozzle while the present jet is injected from a long tube, which makes the jet exit profile significantly different. There also have been some attempts to

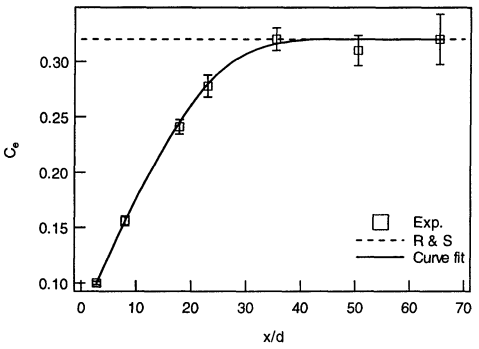

(a)

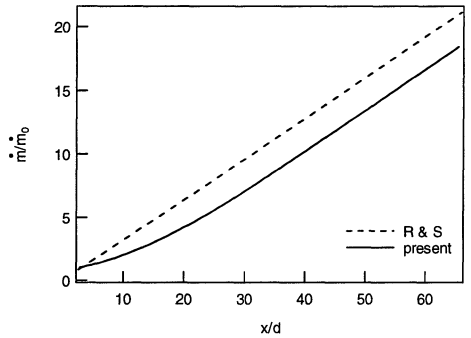

(b)

Figure 3. Entrainment measurement for very slow coflow speed.

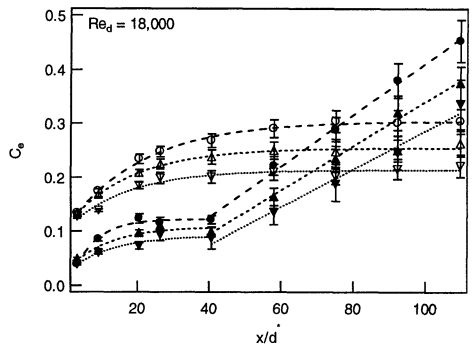

Figure 4. Entrainment coefficient of jets in coflow. See Table 1 for symbols.

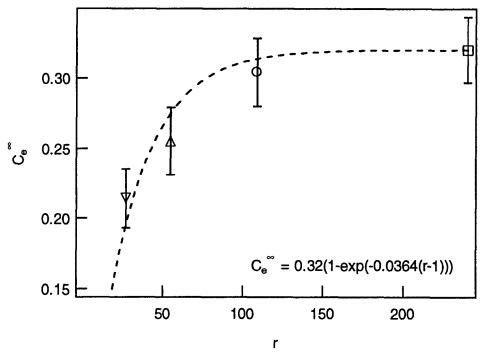

Figure 5. Entrainment coefficient change with the density weighted velocity ratio, r.

measure the entrainment for the jets injected from a long tube. Boguslawski and Popiel (1978) obtained C_e of 0.183 for x/d less than 12, and Trabold et al. (1987) measured C_e of 0.20 for x/d less than 24 for jets injected from long tubes. For our result, the average C_e of 0.120 for x/d less than 12 and 0.185 for x/d less than 24 are obtained, which correspond well with the previous works.

From these observations, we can conclude that the jets injected from a long tube develops slower than the jets from a convergent nozzle, but eventually reaches the same entrainment rate in the far field.

Entrainment of Jets in Coflow

Figure 4 shows the entrainment coefficients measured in different coflow speeds for both reacting and non-reacting cases. For non-reacting cases, the trend is very similar to the entrainment change we observed in the previous section. The non-reacting jet approaches a constant entrainment rate after about 40 jet diameters downstream.

The difference for the jets with different coflow speeds is that the final approaching entrainment rate is reduced as the coflow speed increases. This can be due to the reduced large structure (engulfment) motion with reduced velocity difference of the coflow. Since we know that the entrainment of a non-reacting jet should approach the free jet value for low coflow speed and goes to zero when the coflow speed is the same as the jet speed, we can fit a simple relation to the data, which can be given as,

$$C_e^\infty = 0.32(1- e^{-0.0364(r-1)}) \quad (2)$$

where r is the density weighted velocity ratio between the jet and coflow, $((\rho_0 u_0^2) / (\rho_\infty u_\infty^2))^{1/2}$, and C_e^∞ is the entrainment coefficient after it is fully developed. This relation is shown in Fig. 5.

The same trend can be observed in reacting jets. The increase in coflow speed reduces the overall entrainment.

Effect of Heat Release

In Fig. 4, we can observe a significant reduction in entrainment rate for reacting jets up to about 40 jet diameters downstream compared to non-reacting jets. If we extrapolate the entrainment coefficient value to get the reacting free jet value, we get an entrainment coefficient of about 0.12. Compared to the non-reacting free jet value of 0.32, the reduction is by factor of 2.6. In the same way as the previous section, the entrainment coefficient of a reacting jet after it is fully developed

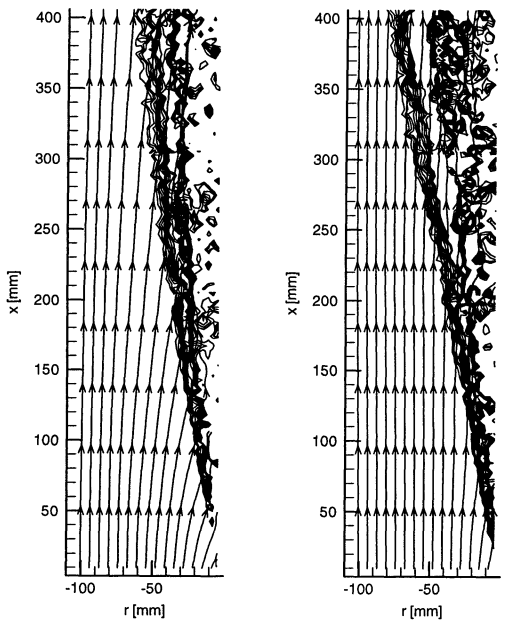

Figure 6. The coflow streamline of averaged velocity field affected by heat release. The RMS v' contour represents the jet boundary.

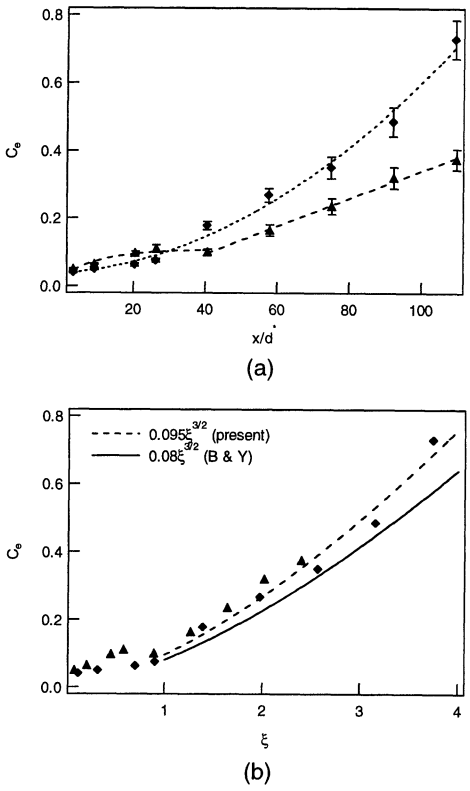

Figure 7. The coflow streamline of averaged velocity field affected by heat release.

in the momentum driven region can be approximated by,

$$C_e^{\infty} = 0.12(1 - e^{-0.0530(r-1)}) \quad (3)$$

Becker and Yamazaki (1978) have obtained $C_e = 0.16$ for the momentum driven reacting jet and modified the equation (1) to include mixing cup density instead of the ambient density. However, this modification cannot entirely explain the present result, since mixing cup density that is 7 times lower than the ambient density is not reasonable in the initial stage of the flame. Therefore, the effect of heat release on the entrainment can be more important than what it is thought to be.

One of the clear examples for the reduction in entrainment by heat release is given by Takagi et al. (1981). They measured the centerline fuel concentration along the axial direction for both reacting and non-reacting cases for jets in coflow and found the initial decay of the fuel concentration is much slower for reacting jets. From our entrainment measurement, we can estimate the entrainment rate using equations (2) and (3) for one of their cases, which give entrainment coefficients of 0.059 and 0.031 for non-reacting and reacting jets respectively. This can explain the reduced concentration decay behavior they observed in the reacting case.

Figure 6 shows the streamlines of the coflow that is being entrained to the jet for both non-reacting and reacting cases which are obtained from the average of over 100 velocity fields. The RMS v' contour represents the jet boundary. The reduction of entrainment in the reacting jet caused by the heat release is obvious.

Effect of Buoyancy

After about 40 jet diameters downstream ($\xi > 1$), the entrainment of reacting jet starts to rise and even surpass the entrainment of the non-reacting jet, Fig. 4. Furthermore, if we observe Fig. 7(a) which shows the entrainment coefficient change with the axial direction for two jets that has almost same density weighted velocity ratio, but different source Reynolds number, the entrainment behavior is different. As the jet develops further downstream, the jet with low source Reynolds number, thus more buoyant jet, has a higher entrainment rate. The increase in entrainment due to the increased buoyancy can be directly observed in the flame length. The flame length gets shorter as the buoyancy increases and thus entrainment increases, which is shown in Table1.

The increase in entrainment due to the buoyancy was also observed by Becker and Yamazaki (1978). They defined a special coordinate ξ, which is based on the Richardson number (Ri_s), to quantify the buoyancy effect. ξ can be expressed as $Ri_s^{1/3} x/d^*$, where Ri_s is given as gd^*/u_0^2. Figure 7(b) shows the same plot as Fig. 7(a), but versus the ξ coordinate. Becker and Yamazaki derived that the entrainment coefficient should

scale with $\xi^{3/2}$ in the buoyant limit, and proposed $C_e = 0.08\xi^{3/2}$ for ξ greater than 2.5. For our data, the expression,

$$C_e = 0.095\xi^{3/2} \quad (4)$$

gives the best fit for ξ greater than 1.0, which is shown in Fig. 7(b). As explained by Becker and Yamazaki, it is not easy to obtain the data for a wide range of ξ, while maintaining high enough Reynolds number for sufficient turbulence. But, since the mixing and temperature at the flame tip can be very important in pollutant generation such as NO_X, it is especially important to obtain a correct relation for entrainment in this region.

Further Considerations

Here, we discuss some additional issues related to the measurement of entrainment. One can define entrainment based upon a cylindrical control volume, where $\dot{m}_{entrained} = -\int v_r 2\pi r dx$ (v_r, radial velocity). We oringinally attempted to use this definition, but as seen in Fig. 6, the reacting case cannot be easily measured using this approach as the streamlines diverge away from the jet. In this case, the entrainment is due to the growth of the jet boundary into the coflow. This suggests the use of a tapered cylinderical control volume with the side defined by the jet boundary, which is the approach used above.

CONCLUSIONS

The entrainment properties of non-reacting and reacting jets in coflow are investigated. The results can be summarized as follows.

1. The direct entrainment measurement method using PIV is developed and tested by the comparison with previous data on free jets. This method effectively avoids the difficulties caused by heat release and density fluctuations in reacting jets. The major uncertainty of the method is related to the determination of the jet boundary and its angle.

2. Jets originating from a long tube develops slower than the jets from a nozzle, but eventually reach the same entrainment rate. The entrainment rate settles down to a constant value within 35 to 40 jet diameters.

3. The increase in coflow speed reduces the entrainment, which is thought to be caused by the reduced large structure motion. The entrainment coefficient can be fitted to an exponential relation by introducing the density weighted velocity ratio.

4. The effect of heat release reduces the entrainment in the near field of reacting jets by factor of 2.6. This effect is more significant than be explained by the change in mixing cup density. This effect is especially important in the initial decay of the fuel concentration which can possibly have important effects on overall chemistry.

5. The effect of buoyancy increases the entrainment to compensate the effect of heat release in the nearfield of the jet. For ξ greater than 1.0, the entrainment coefficient increases with $\xi^{3/2}$.

ACKNOWLEDGEMENTS

This work is sponsored by the Gas Research Institute, with R. V. Serauskas as technical monitor. The authors gratefully acknowledge valuable discussions with L. Muñiz, E. F. Hasselbrink and L. K. Su. D. Han acknowledges the support of the Stanford Graduate Fellowship program (Mr. and Mrs. Benhamou Fellow).

REFERENCES

Becker, H. A. and Yamazaki, S., 1978, "Entrainment, Momentum Flux and Temperature in Vertical Free Turbulent Diffusion Flames," Combustion and Flame, Vol. 33, pp. 123-149.

Boguslaski, L. and Popiel, C. O., 1979, "Flow Structure of the Free Round Turbulent Jet in the Initial Region," J. of Fluid Mechanics, Vol. 90, part 3, pp. 531-539.

Broadwell, J. E. and Lutz, A. E., 1998, "A Turbulent Jet Chemical Reaction Model: NO_X Production in Jet Flames," Combustion and Flame, Vol. 114, pp. 319-335.

Hasselbrink, E. F., 1999, "Transverse Jets and Jet Flames : Structure, Scailing and Effects of Heat Release," Ph.D. Thesis, Stanford University, Stanford, CA.

Hill, B. J., 1972, "Measurement of Local Entrainment Rate in the Initial Region of Axisymmetric Turbulent Air Jets," J. Fluid Mechanics, Vol. 51, part 4, pp. 773-779.

Muñiz, L., 1999, "Particle Image Velocimetry Studies of Turbulent Non-Premixed Flames," Ph.D. Thesis, Stanford University, Stanford, CA.

Westerweel, J., 1997, "Fundamentals of Digital Particle Image Velocimetry," Meas. Sci. Technol., Vol. 8, pp. 1379-1392.

Westerweel, J., Dabiri, D. and Gharib, M., 1997, "The Effect of a Discrete Window Offset on the Accuracy of Cross-Correlation Analysis of Digital PIV Recordings," Experiments in Fluids, Vol. 23, pp. 20-28.

Ricou, F. P. and Spalding, D. B., 1961, "Measurements of Entrainment by Axisymmetrical Turbulent Jets," J. Fluid Mechanics, Vol. 11, pp. 21-32.

Takagi, T., Shin, H. and Ishio A., 1981, "Properties of Turbulence in Turbulent Diffusion Flames," Combustion and Flame, Vol. 40, pp. 121-140.

Trabold, T. A., Esen, E. B. and Obot, N. T., 1987, "Entrainment by Turbulent Jets Issuing from Sharp-Edged Inlet Round Nozzles," J. Fluids Engineering, Vol. 109, pp. 248-254.